Boron recovery from seawater with a new low-cost adsorbent material

H. Demey, Thierry Vincent, M. Ruiz, M. Nogueras, A. M. Sastre, E. Guibal

Boron recovery from seawater with a new low-cost adsorbent material

H. Demey [a,b,*], T. Vincent [b], M. Ruiz [a], M. Nogueras [a], A.M. Sastre [c], E. Guibal [b]

[a] Universitat Politècnica de Catalunya, Department of Chemical Engineering, EPSEVG, Av. Víctor Balaguer, s/n, 08800 Vilanova i la Geltrú, Spain
[b] École des Mines d'Alès, Centre des Matériaux des Mines d'Alès, 6 Avenue de Clavières, F-30319 Alès CEDEX, France
[c] Universitat Politècnica de Catalunya, Department of Chemical Engineering, ETSEIB, Diagonal 647, 08028 Barcelona, Spain

ABSTRACT

A new adsorbent [chiFer(III)] for boron recovery from seawater was prepared using chitosan and iron(III) hydroxide. Experiments were carried out in a column system. Seawater samples were collected from the Mediterranean Sea off the coast of Vilanova i la Geltru, Spain (coordinates: 41.18; 1.75). Several adsorption–desorption cycles were performed to evaluate the efficiency of the adsorbent, and a desorp-tion step was carried out using MilliQ-water of pH 12 (0.01 M NaOH solution). The molar ratio between the mass of adsorbed boron in the five consecutive cycles and the mass of iron(III) hydroxide present in
the adsorbent beads was 10.7 $mmol_B \cdot (mol_{Fe(OH)_3})^{-1}$. The experimental results were evaluated using the Thomas, Yoon and Nelson, and Bohart–Adams models, which fitted the experimental data adequately. The adsorbent was characterized by SEM-EDX analyses and BET surface; porosity studies confirmed that the chiFer(III) composite is a mesoporous material.

HIGHLIGHTS

- A new composite containing chitosan and iron(III) hydroxide has been manufactured.
- SEM-EDX analysis revealed a homogenous distribution of $Fe(OH)_3$ in whole material.
- An adsorption column system was used for boron recovery from seawater.
- Adsorption–desorption cycles were performed and desorption uptake remained >40%.
- Elution was efficiently eluted with water at pH 12.

GRAPHICAL ABSTRACT

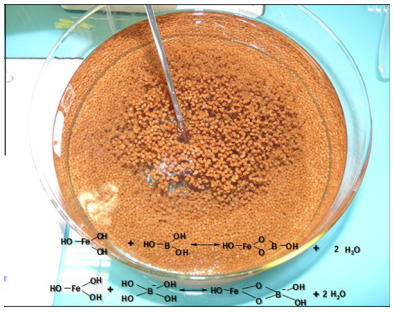

Keywords:
Chitosan
Iron(III)
Boron
Seawater
New sorbent

1. Introduction

Water is essential to the survival of humans, animals and plants and has played a major role in human behavior throughout the history of mankind; scarcity of water in particular regions led to forced migrations and, in the most extreme cases, is thought to have been responsible for the disappearance of ancient cultures. The increasing demand for potable water is a pressing concern, and although Earth is composed mainly of water, only 1% of this is consumable fresh water. Therefore, the search for advanced seawater treatment mechanisms is very important for human survival.

Boron is a mineral present in seawater. It belongs to group 13 of the Periodic Table and has two stable isotopes, B_{10} and B_{11}. This study considers boron in terms of the health risks highlighted by the World Health Organization (WHO), on the basis of a study in which short- and long-term oral exposure to boric acid or borax

* Corresponding author at: Universitat Politècnica de Catalunya, Department of Chemical Engineering, EPSEVG, Av. Víctor Balaguer, s/n, 08800 Vilanova i la Geltrú, Spain. Tel.: +34 938937778; fax: +34 934017700.
E-mail address: hary.demey@upc.edu (H. Demey).

in laboratory animals was found to cause toxicity that consistently targeted the male reproductive tract. Testicular lesions have been observed in rats, mice and dogs given boric acid or borax in food or drinking-water, and a guide level of 2.4 mg L^{-1} has been recommended in drinking water [1].

According to Österk et al. [2], the ingestion of large amounts of boron can affect the central nervous system and the reproductive system in humans. Although small quantities of boron are important for plant growth, high levels are harmful to most species [3]. The maximum recommended boron concentration in irrigation waters varies considerably according to the type of plant: lemon and blackberry plants cannot tolerate boron concentrations greater than 0.5 mg L^{-1} (extremely sensitive plants); orange, peach, cherry, plum, onion, and grape can only tolerate boron concentrations of up to 0.75 mg L^{-1} (very sensitive plants); but sorghum, cotton, celery and asparagus can tolerate boron concentrations of up to 10 mg L^{-1} (very tolerant plants) [3].

Currently there is no simple method for removing boron from seawater. Nevertheless, several methodologies have been used for boron removal from aqueous solutions, such as adsorption with clays [4], fly ash [5], ion exchange with boron-specific resins [6,7], reverse osmosis [8–10], electrodialysis [11], precipitation [12], chemical coagulation and electrocoagulation [13].

Reverse osmosis (RO) technology has been widely used over the last decade to desalinate water [3]. However, a specific problem is encountered in the removal of boron compounds: the use of a multi-pass reverse osmosis membrane and the modification of pH are needed for better boron separation, which increase the cost of desalination plants. RO is usually combined with ion-exchange to effectively separate boron from seawater [3]; effective ion-exchange resins (with N-methyl-D-glucamine as functional groups) have been used in a second purification stage, but these resins are also costly to regenerate.

Different materials have been reported in the literature as inexpensive sorbents for boron removal; for example, calcium alginate beads have been found by Demey et al. [14] and Ruiz et al. [15,16] to be effective for boron recovery from aqueous solutions (biosorption) at high pH (pH > 9). Layered double hydroxide (LDH) materials synthesized by co-precipitation have been evaluated by Ferreira et al. [17]: Mg/Al and Mg/Fe-LDHs. It was found that the mechanism governing boron removal on Mg/Fe-LDH was basically adsorption rather than a combination of anion exchange and adsorption on external surface (on Mg/Al-LDH); maximum boron removal was 92% for Mg/Al-LDH and 33% for Mg/Fe-LDH.

Despite the good boron uptake of LDHs (as demonstrated by Koilraj and Srinivasan [18]), some drawbacks were detected by Ferreira et al. [17]: metal ion release was greater into the solution using Mg/Al-LDH than the solution using Mg/Fe-LDH. Studies by Yoshioka et al. [19] also confirmed a partial dissolution of Mg/Al-LDH (prepared by co-precipitation and thermally activated at 500 °C) upon removal of tetraflouroborate ions; 10% of the initial magnesium content in the material (4:1, Mg/Al) was found to dissolve into the solution (until 3.6:1), apparently due to the formation of a soluble complex with F^- and boron species. Similar conclusions were reported by Koilraj and Srinivasan [18] using Zn_2Al-Cl-CLDH: below pH 4 and above pH 11, the sorbent was very unstable owing to leaching of Zn^{+2} and Al^{+3} ions into the solution [18].

Zhang and Reardon [20], using hydrocalumite ($Ca_4Al_2(OH)_{12}(OH)_2 6H_2O$) and ettringite ($Ca_6Al_2(OH)_{12}(SO_4)_3 26H_2O$) for the removal of oxyanions (including tetrahydroxy-borate $B(OH)_4^-$ ions) from aqueous solution, found that neutral boric acid is not easily adsorbed by LDHs in acidic conditions; the best results are generally achieved in basic conditions because of the high pH-buffering capacity, which strongly increases the final pH of the solutions [21]. This is an obvious constraint on the use of these materials in certain applications, especially for boron recovery from seawater. As such, further research is needed to improve the stability of these materials in order to optimize the benefits of their adsorption uptake at neutral pH. Theiss et al. [21] also note that there are few studies on boron desorption (regeneration of LDH-sorbents) and few studies carried out in continuous system applications (rather than small-scale batch systems) [21].

Therefore, in this study a new low-cost adsorbent has been manufactured for boron recovery from seawater. The adsorbent is a composite of chitosan and iron(III) hydroxide [chiFer(III)], in which chitosan acts as a matrix (hybrid polymeric/inorganic material). Previous studies have reported the use of hydroxides to remove boron from aqueous solutions: Turek et al. [22] used $Ni(OH)_2$, $Zn(OH)_2$, $Co(OH)_2$, $Mg(OH)_2$, $Fe(OH)_3$ and $Al(OH)_3$ for the adsorption/co-precipitation of boron from aqueous solutions.

A good sorbent, especially for large-scale application, must be recyclable in order to be competitive. Turek et al. [22] reported a boron removal percentage (from aqueous solutions) greater than 40% using $Fe(OH)_3$, but no desorption data were presented; standard chitosan-based spherical beads can improve the handling of the active material [$Fe(OH)_3$] and improve the adsorption–desorption process. This study reports the preparation of a new chitosan-based composite to improve the handling of $Fe(OH)_3$ as an adsorbent to recover boron from seawater in a continuous system. Reuse of the adsorbent was evaluated in several adsorption–desorption cycles, and the Thomas [23], Yoon and Nelson [24,25], and Bohart–Adams [26] models were used to fit the experimental results.

2. Experimental

2.1. Materials

Boron solutions were prepared using boric acid ($B(OH)_3$) provided by Merck AG (Germany). Iron(III) chloride hexahydrate used for sorbent preparation was provided by Panreac (France). Chitosan was supplied by Aber Technologies (France), and its molecular weight (125,000 g mol^{-1}) was previously reported by Ruiz et al. [27] using Size Exclusion Chromatography (SEC) coupled with light scattering and refractometry. The degree of deacetylation determined by Fourier Transform Infrared (FTIR) spectroscopy was found to be 87% [28].

2.2. Preparation of chiFer(III) composite microspheres

A chitosan solution was prepared by dissolving 1 g of chitosan in 1% w/w acetic acid solution and stirring for at least 3 h. Twenty grams of $FeCl_3 \cdot 6H_2O$ powder were mixed in 60 mL of HCl solution (1 M) until complete dissolution. The chitosan solution (640 g, 1% w/w) was then mixed with iron(III) solution under vigorous stirring (600 rpm) for 120 min.

The chitosan–iron(III) solution was added drop-by-drop with a peristaltic pump through a thin nozzle (Ø 1.6 mm) into an aqueous solution of 1 M sodium hydroxide under magnetic stirring to produce microspheres of the composite chitosan/iron(III) hydroxide [chiFer(III)].

The composite particles were kept under stirring for 6 h at room temperature (25 °C) and then filtered and washed intensively with distilled water to remove the excess iron on the surface of the composite beads. The standard wet beads used in this study had an average diameter of 2.0 mm and are shown in Fig. 1.

2.3. Characterization of sorbents

2.3.1. BET surface area and porosity of chiFer(III)

Nitrogen adsorption apparatus (Micrometrics, TriStar 3000) was used to determine the porosity and specific surface area. In order to

Fig. 1. A new chitosan/Fe(OH)$_3$-based sorbent for boron removal.

compare the influence of drying method on porosity, the samples were dried using two different methods: (i) air drying (ordinary method), in which the wet beads of chiFer(III) (the standard adsorbent used in this study) were washed with ethanol and then kept at room temperature (20 °C) for 48 h to dry, giving an average air-dried bead diameter of 0.85 mm; and (ii) freeze drying, in which the adsorbent was dried with a freeze dryer (Bioblock scientific, Christ) at 223 K and 0.01 mbar. The hydration ratio, calculated as the amount of water (g) in wet beads (standard material) relative to the total amount of chiFer(III) composite in grams (wet weight), was 92.7% w/w.

Dried samples were degassed with N_2 at 100 °C for 6 h prior to experiments to clean the adsorbent surface [29]. The surface area, pore volume and pore diameter of the adsorbent were determined by N_2 adsorption at 77 K using the BET method [30], and the pore size distribution was determined using the Barret–Joyner–Halenda (BJH) model [31].

2.3.2. Scanning electron microscopy

Samples were analyzed using a Quanta FEG 200 environmental scanning electron microscope (ESEM), a specialized high-performance scanning electron microscope (SEM) with low-vacuum, high-vacuum and "Environmental SEM" modes, capable of analyzing samples under pressures of up to 6.6×10^{-3} bar. The microscope is also equipped with an Oxford INCA Energy Dispersive X-ray (EDX) system for chemical analysis.

The adsorbent samples were analyzed before and after boron adsorption. Though the boron signal was too low to be measured, SEM-EDX analysis was used to detect the main elements present at the surface of sorbent particles.

2.4. Collection and characterization of seawater samples

Seawater samples were collected from the Mediterranean Sea at the Expandable Seafloor Observatory (OBSEA) in Vilanova i la Geltrù, Spain. This submarine observatory is located 4 km off the Vilanova i la Geltru coast (coordinates: 41.18; 1.75) in a fishing protected area at a depth of 20 m. It is connected to the coast by a mixed energy and communication cable.

The main advantages of a cabled observatory are the uninterrupted power supply to scientific instruments and the high-bandwidth communication link, which guarantee the availability of real-time data and prevent the problems associated with battery-powered systems. The solution proposed for this study is an optical Ethernet network that transmits data continuously to marine sensors connected to the observatory, making OBSEA capable of performing real-time observation of multiple parameters in the marine environment.

OBSEA is equipped with a CTD (SBE 16 plus V2 Seacat, Sea-Bird Electronics, Inc.) to measure conductivity, temperature and pressure in real time. These parameters can be used to obtain the variation in seawater salinity as a function of time; a pH sensor (Honeywell Durafet 07777 DVP) was also fitted to monitor the pH throughout whole year. Samples were collected from the measurement point where the CTD is installed by divers who submerge to the submarine platform periodically with a 10 L Niskin bottle (Model 1010X NISKIN-X).

2.5. Continuous sorption system

Five consecutive adsorption–desorption cycles were carried out using a dynamic system to obtain information about the column performance. Wet beads of chiFer(III) were used as adsorbent. A glass column with a diameter of 2.6 cm and a length of 15 cm was employed. The column was packed with 7.2 g of chiFer(III) (dried weight). The seawater (boron concentration of 4.2 mg.L^{-1}, pH 8.3) was delivered by up-flow to the column at 20 °C using a peristaltic pump at a flow rate of 0.3 mL min^{-1}. Samples of 6 mL were collected using a Gilson FC 203B fraction collector (United Kingdom).

Consecutively, the adsorbent packed in the column was eluted and the adsorbed boron was recovered using Milli-Q water at pH 12 (NaOH 0.01 M solution) for 48 h at a flow rate of 0.3 mL min^{-1}. Samples were periodically collected and analyzed for outlet boron concentration. After each cycle, the adsorbent was rinsed with distilled water (pH 7) before being reused to remove the excess NaOH solution remaining in the column. The efficiency of boron adsorption and desorption in the repeated cycles was determined by applying Eqs. (1) and (2):

$$\%\text{Adsorption} = \frac{m_{ad}}{m_0} \cdot 100 = \frac{m_0 - m_{eff}}{m_0} \cdot 100 \quad (1)$$

$$\%\text{Desorption} = \frac{m_d}{m_{ad}} \cdot 100 \quad (2)$$

where m_0 is the mass of boron at the column inlet (g), m_{ad} is the mass of adsorbed boron (g), m_{eff} is the mass of boron in the effluent (g) at any time, and m_d is the mass of desorbed boron (g). The mass of adsorbed boron and mass of desorbed boron were calculated from the area below the adsorption and elution curves, respectively.

2.6. Modeling of breakthrough curves

Breakthrough curves can be used to depict the adsorption process in an experimental column system. Here, the breakthrough curves show the loading behavior of the boron to be recovered, which is defined as the ratio of effluent boron concentration, C_t (mg L^{-1}), to inlet boron concentration, C_0 (mg L^{-1}), (C_t/C_0), as a function of time, t, or volume of effluent (mL) for a given height.

The experimental sorption capacity q_{exp} (mg g^{-1}) can be obtained using Eq. (3); it is calculated from the area under the breakthrough curve, taking into account the volume of seawater through the column and the mass of adsorbent, m (g), used in the packed column.

$$q_{exp} = \int_0^{V_{total}} \frac{(C_0 - C_t)}{m} dV \quad (3)$$

2.6.1. Thomas model

There are many dynamic models for describing the performance of column systems. The Thomas model is widely used for its simplicity and for its adequate accuracy in predicting breakthrough

curves under various operating conditions. The model is represented by the following equation [32]:

$$\frac{C}{C_0} = \frac{1}{1 + \exp[K_T(q_T m - C_0 V)/Q]} \quad (4)$$

where K_T is the Thomas rate constant (L min^{-1} mg^{-1}), m is the mass of sorbent (g), Q is the volumetric flow rate (L min^{-1}), C is the sorbate concentration and q_T is the Thomas sorption capacity (mg g^{-1}). The linearized form of the Thomas model is expressed in Eq. (5):

$$\ln\left(\frac{C}{C_0} - 1\right) = \frac{K_T Q_T m}{Q} - \frac{K_T C_0}{Q} V \quad (5)$$

In addition, since time (min) is calculated as $t = V/Q$, Eq. (5) can be expressed as follows:

$$\ln\left(\frac{C}{C_0} - 1\right) = \frac{K_T Q_T m}{Q} - K_T C_0 t \quad (6)$$

The sorption capacity q_T and Thomas constant K_T can be determined by plotting $[(C/C_0) - 1]$ against t (min).

2.6.2. Yoon and Nelson model

The Yoon and Nelson model is a simple model for describing the sorption and breakthrough of the sorbate. It requires no detailed data on the characteristics of the sorbate, the type of sorbent, or the physical properties of the sorption bed, and is expressed as follows [32]:

$$\frac{C}{C_0} = \frac{\exp(K_{YN} t - \tau K_{YN})}{1 + \exp(K_{YN} t - \tau K_{YN})} \quad (7)$$

The linearized form is described by the following equation:

$$\ln \frac{C}{C_0 - C} = K_{YN} t - \tau K_{YN} \quad (8)$$

where τ is the time required for 50% sorbate breakthrough (min) when boron concentration C (mg L^{-1}) is one half of C_0, and K_{YN} is the rate constant. K_{YN} and τ can be determined from $\ln[C/(C_0 - C)]$ against t plots. According to the model, the amount of boron sorbed is one half of the initial boron concentration passed through the fixed-bed column within 2τ (Eq. (9)) [32]:

$$q_{YN} = \frac{1}{2m}[C_0 Q(2\tau)] = \frac{C_0 Q \tau}{m} \quad (9)$$

where q_{YN} is the sorption capacity (mg g^{-1}), and m is the mass of sorbent (g).

2.6.3. Bohart–Adams model

The Bohart–Adams model was originally applied to a gas–solid system in 1920 [26] but is widely used in liquid–solid systems to describe breakthrough curve performance [33,34]. It assumes that sorption rate is proportional to the residual capacity of the solid and the sorbate concentration [14]:

$$\frac{C_t}{C_0} = \frac{\exp[k_{BA} C_0 t]}{\exp\left[\frac{k_{BA} N_0 Z}{\upsilon}\right] - 1 + \exp[k_{BA} C_0 t]} \quad (10)$$

where t is the service time of the breakthrough curve (min), N_0 is the volumetric sorption capacity (mg L^{-1}), k_{BA} is the kinetic constant (L mg^{-1} min^{-1}), Z is the depth of the bed (cm), C_0 (mg L^{-1}) is the initial boron concentration, C_t (mg L^{-1}) is the effluent boron concentration and υ is the superficial flow velocity (cm min^{-1}). The linearized form of the Bohart–Adams model can be expressed as follows:

$$\ln\left[\frac{C_0}{C_t} - 1\right] = \ln\left[\exp\left(\frac{k_{BA} N_0 Z}{\upsilon}\right) - 1\right] - k_{BA} C_0 t \quad (11)$$

In Eq. (11), k_{BA} can be obtained from the slope of the plot $\ln[C_0/C_t - 1]$ versus breakthrough time t, and N_0 is obtained from the intersection with the axis at time $t = 0$. In this study, experimental data were fitted mathematically to the Thomas, Yoon and Nelson, and Bohart–Adams models.

3. Results and discussion

3.1. Characterization of sorbent and seawater

3.1.1. Scanning electron microscopy

Fig. 2 shows the spherical topography of the sorbent material (Fig. 2a): the particles have an average diameter of 2 mm. Small cavities can be seen across the entire surface of the material (Fig. 1b). Fig. 1c shows the cross-section surface of freeze-dried adsorbent. EDX-analysis of different zones of the cross-section (Fig. 1c and d) suggests that the elements are homogeneously distributed in the chiFer(III) composite. Indeed, Fe(III) element (tracers of the active component, i.e. $Fe(OH)_3$) and C and O elements (tracers of the encapsulation material, i.e. chitosan) were detected in the same magnitude in the different zones of the cross-section area, suggesting that encapsulation with chitosan is an innovative and efficient technique for the immobilization of active materials. The mass percentage of $Fe(OH)_3$ distributed throughout the dried adsorbent was 47.9% w/w.

By contrast, Fig. 3 shows the SEM images of chiFer(III) dried by air drying at room temperature (ordinary method). The influence of the drying method can be seen on the surfaces of the chiFer(III) material: particles have an average diameter of 0.85 mm, after drying (Fig. 3a); folds are observed over the entire surface (Fig. 3b); and small cavities or pores can be seen between these folds (Fig. 3c), which do not appear to be easily accessible.

3.1.2. BET surface area and porosimetry

Nitrogen adsorption–desorption isotherms for chiFer(III) samples (dried by two different methods) are shown in Fig. 4a and b; the hysteresis loops observed in both figures follow the same trend. According to the IUPAC classification, the loops are of type H3. The shape of hysteresis loops has often been identified with specific pore structures; according to Sing et al. [29], the H3 loop does not exhibit any limiting adsorption at high P/P_0 and is observed with aggregates of plate-like particles, giving rise to slit-shaped pores [29]. It is often associated with large pore channels and indicates the presence of mesopores.

The pore size distributions calculated from the desorption branch of isotherms are also presented in Fig. 4a and b. The BET surface area, average pore diameter and average pore volume of freeze-dried beads are 37.3 m^2 g^{-1}, 21.5 nm and 0.2 cm^3 g^{-1}, respectively. The results confirm that the chiFer(III) composite is a mesoporous material (2 nm < pore size < 50 nm).

As shown in Figs. 2 and 3, the surface topography of the chiFer(III) composite is substantially affected by the drying method [35,36]. The freeze-dried beads conserve a largely similar structure to the hydrated form. By contrast, the air-drying method (at room temperature) does not preserve the original surface topography of the samples; instead, a series of folds in the form of wrinkles can be seen, which hinder access to a percentage of the pores (which cannot be detected by the BET method). In addition, when the adsorbent is air-dried, a portion of the adsorbed water remains in the inter-particle space. During the degassing process (before BET measurements), elimination of the adsorbed water results in a surface that is inaccessible to N_2 molecules. Consequently, the pore size distribution of the air-dried material (Fig. 4a) is quite low, which can be attributed to the degassing process rather than drying step and is not comparable to the results of the freezing-drying method.

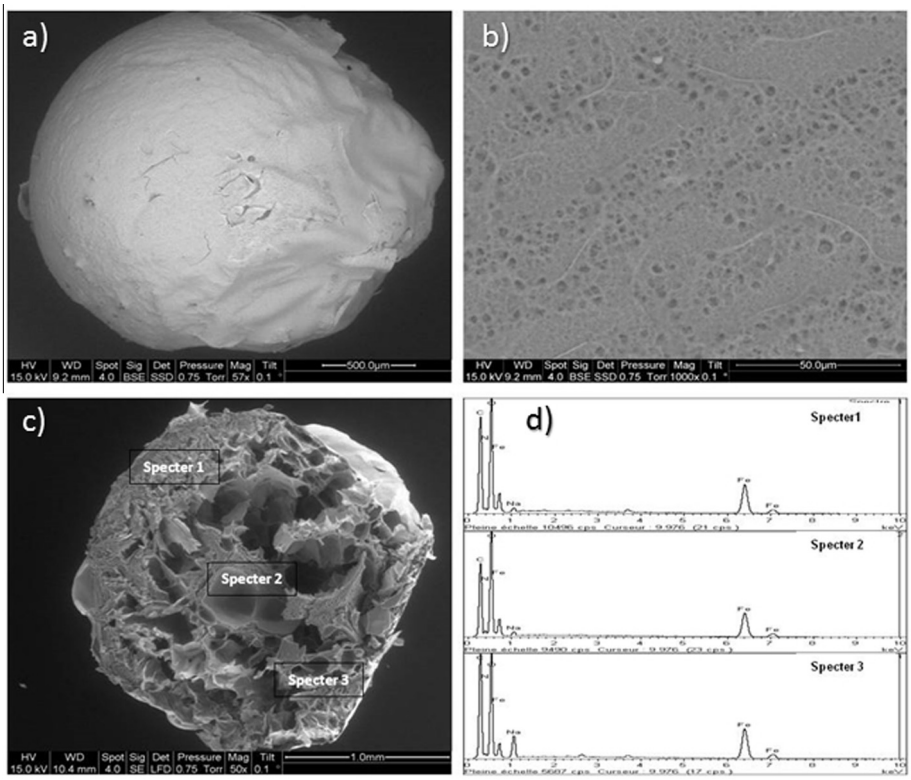

Fig. 2. SEM images of freeze-dried chiFer(III). (a) Topography of chiFer(III) composites. (b) Surface of chiFer(III) composites. (c) Cross-section of the freeze-dried adsorbent. (d) EDX-analysis of the cross-section of the adsorbent.

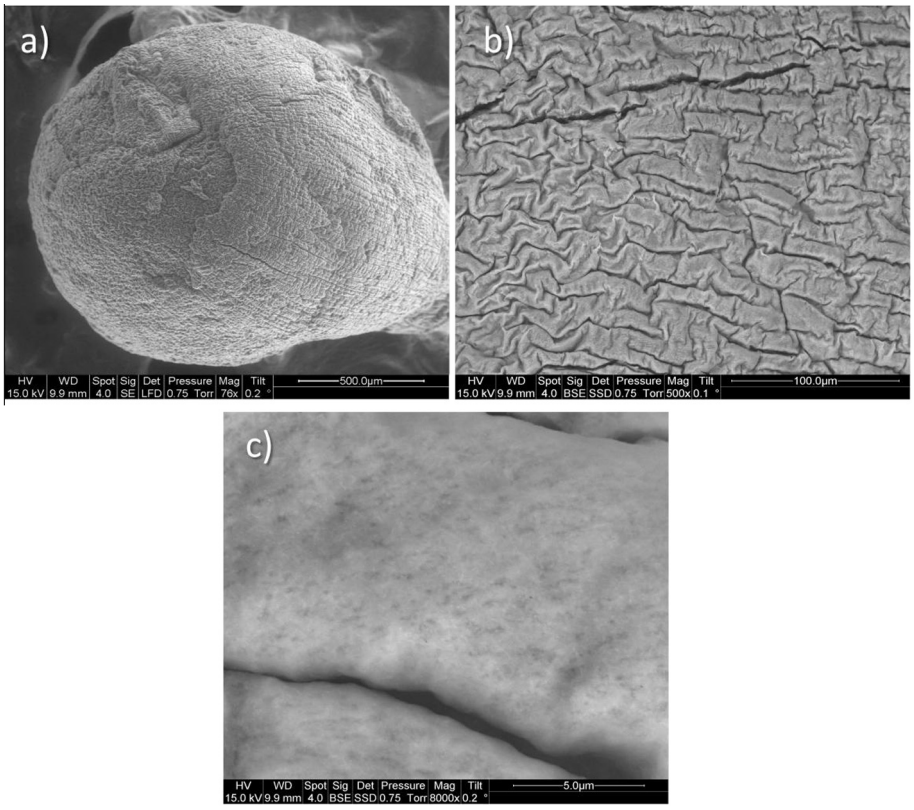

Fig. 3. SEM images of air-dried chiFer(III). (a) Topography of chiFer(III) composites. (b) Surface of chiFer(III) composites. (c) View of folds over the surface of air-dried chiFer(III).

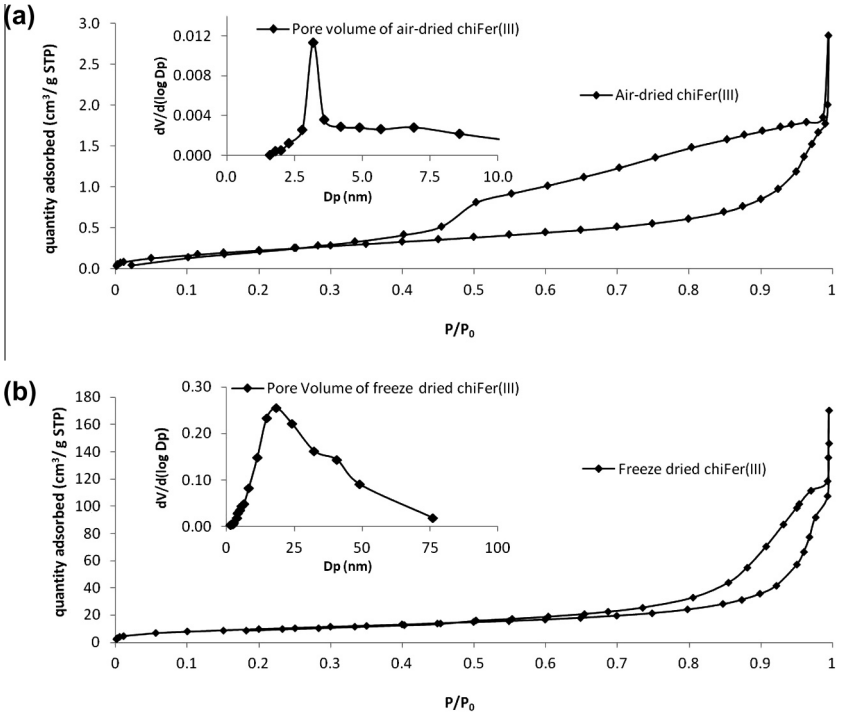

Fig. 4. N_2 adsorption–desorption isotherms and pore distribution of chiFer(III) composite. (a) ChiFer(III) material dried by air drying at room temperature. (b) Freeze-dried chiFer(III).

3.1.3. Seawater characterization

Salinity values were provided by OBSEA. Figs. SM1 and SM2 (of Supplementary Materials section) show the variations in the temperature (Fig. SM1a), salinity (Fig. SM1b), pH (Fig. SM1c), conductivity (Fig. SM2a) and pressure (Figure SM2b) of seawater as a function of time. The average pH and salinity, monitored over a one-month period, were 8.3 and 38 psu, respectively. Salinity values were verified in the chemical engineering laboratory of the Polytechnic University of Catalonia using an EC-215 conductivity meter (PCE-instruments). The boron concentration of samples was measured using ICP-AES (HORIBA JOBIN YVON, France) with a wavelength of 249.7 nm; boron concentration in seawater was 4.2 mg L^{-1}, which is consistent with the values reported in the literature [3].

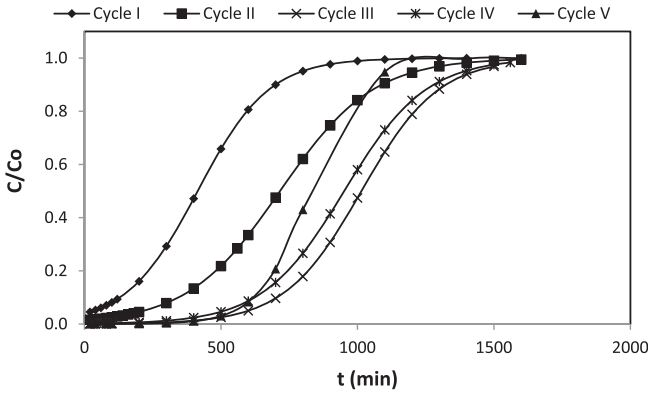

Fig. 5. Boron adsorption cycles using chiFer(III) as adsorbent.

3.2. Adsorption–desorption cycles

In order to demonstrate the re-usability of the chiFer(III) composite, the sorption–elution–washing–sorption cycle was repeated five times. Breakthrough curves generally permit a good description of the processes in adsorption columns; the resulting breakthrough curves are given in Fig. 5.

The sorption capacity values of the column for each cycle are shown in Table 1; the Thomas, Yoon and Nelson, and Bohart–Adams models show a good fit with the experimental data. The breakthrough capacity of chiFer(III) increased to some extent during the second cycle and began to decrease from fourth and fifth cycles. In the second cycle the sorption capacity reached 0.13 mg g^{-1}, due to two factors: (i) Functional sites on the adsorbent were activated by reconditioning with NaOH solution during the elution step. A similar trend was obtained by Ennil-Köse and Österk, [37] and by Badruk et al. [38]; (ii) In the production of the chiFer(III) composite, the reaction time may have been too short to allow all of the Fe^{+3} ions (present in the composite) to react with OH^- groups, as a result of which the remaining Fe^{+3} reacted in the first elution step in the column (performed with 0.01 M NaOH solution), increasing the sorption capacity in the next consecutive cycle (second cycle). From the fourth cycle, the adsorption capacity began to decrease as the packed adsorbent became saturated. The Thomas, Yoon and Nelson, and Bohart–Adams models fitted the experimental data adequately, and no significant differences were found between models.

In the operating conditions used in this study, the molar ratio between boron and $Fe(OH)_3$ was determined as the ratio between the total amount of sorbed boron in the five adsorption cycles (mmol) and the total mass of $Fe(OH)_3$ (mol) present in the adsorbent beads. The resulting value is 10.7 $mmol_B \cdot (mol_{Fe(OH)_3})^{-1}$.

The main conclusion of this study is that the new low-cost adsorbent presented can be used at least five times for boron recovery from seawater and elution can be performed using water at pH 12. This can be correlated to the fact that, in basic solutions, the electrostatic interaction between chitosan–metal hydroxide composites and boron is much weaker and the adsorbed boron

Table 1
Boron adsorption capacities of several adsorption–desorption cycles and parameters of Thomas, Yoon and Nelson and Bohart–Adams models on experimental data (±standard error).

Cycle	Experimental		Thomas parameters			Yoon and Nelson parameters			Bohart–Adams parameters			
	q_{exp} (mg g^{-1})	Adsorption (%)	K_T 10^3 (L min^{-1} mg^{-1})	q_T (mg g^{-1})	r^2	K_{YN} 10^3 (min^{-1})	T (min)	q_{YN} (mg g^{-1})	r^2	K_{BA} 10^3 (L mg^{-1} min^{-1})	N_0 (mg L^{-1})	r^2	Elution (%)
1	0.08	28.9	1.88 ± 0.09	0.07 ± 0.01	0.999	7.70 ± 0.07	415 ± 20	0.07 ± 0.01	0.999	1.83 ± 0.07	6.6 ± 0.1	0.9997	99.8
2	0.13	49.7	1.40 ± 0.07	0.13 ± 0.01	0.841	6.60 ± 0.1	718 ± 36	0.12 ± 0.01	0.834	1.40 ± 0.09	11.4 ± 0.8	0.841	42.8
3	0.12	40.0	1.69 ± 0.08	0.17 ± 0.02	0.733	7.10 ± 0.1	1015 ± 55	0.18 ± 0.02	0.732	1.76 ± 0.10	16.1 ± 0.9	0.8376	42.9
4	0.10	39.5	1.59 ± 0.08	0.16 ± 0.02	0.678	6.70 ± 0.5	952 ± 50	0.16 ± 0.02	0.679	1.60 ± 0.10	15.1 ± 1	0.6787	40.2
5	0.09	38.0	2.52 ± 0.13	0.12 ± 0.01	0.875	10.60 ± 0.1	827 ± 40	0.12 ± 0.01	0.750	2.52 ± 0.20	13.1 ± 1	0.750	29.8

leaves the adsorption sites of the adsorbent. This a great advantage over other commercial sorbents such as ion-exchange resins, which require more expensive eluents for sorbent regeneration (for example, 0.5 M HCl for Dowex 2x8 resins [37] and 5% H_2SO_4 [39] for Diaion CRB 02 resins). Boron recovery from the loaded sorbent was greater than 40% in the first four successive cycles and began to decrease from fourth cycle (Table 1).

Fig. 6 shows the volume of dilute NaOH solution (water at pH 12) required to regenerate the adsorbent; in all cycles, recovered boron was concentrated in the same elution solution (and the pH was adjusted to 12 between each cycle). The required volume was normally 300 mL (Fig. 6); the first cycle required a higher volume (>700 mL) because the Fe^{+3} ions present in the sorbent (which did not react with NaOH in the chiFer(III) preparation) react with NaOH in the first desorption step.

Boron speciation is dependent on pH and concentration. In dilute solutions boric acid is monomeric, but at a concentration above 0.1 M polymeric species become significant. Eq. (12) reports the dissociation reaction of boric acid (monomeric form) ($K_a = 5.80 \times 10^{-10}$ mol L^{-1}). According to Demey et al. [40], the relative concentration of the $B(OH)_4^-$ anion increases with increasing pH until it becomes the dominant species at a pH of approximately 9.2. The formation of this species is a direct result of the tendency of boron to form complexes with electron–donor species including oxygen (present on borate anions). In dilute neutral solutions, boric acid represents more than 99% of total boron [41]. Boric acid is a Lewis acid and can bind a hydroxyl ion, forming the borate anion.

$$B(HO)_3 + H_2O \leftrightarrow B(OH)_4^- + H^+ \quad (12)$$

Two mechanisms can take place in boron adsorption on metal hydroxides: (i) the first is related to the electrostatic forces, as proposed by Zelmanov and Semiat [42], who reported that the pH_{PZC} of iron(III) hydroxide is 8.7, so at pH < pH_{PZC} the surface of the sorbent is positively charged, indicating a greater affinity for anions [$B(OH)_4^-$], whereas at pH > pH_{PZC} the surface becomes negatively charged and adsorption is favourable for $B(OH)_3$ species; (ii) the second was reported by Wang et al. [43], and demonstrated by Demey et al. [40] and Ruiz et al. [15], where the interaction between the hydroxyl groups of the metal hydroxide with the OH^- groups of boron species occurs similarly to an esterification reaction (Eqs. (13) and (14)). Although it is not a conventional esterification, it can be related to this process. Both boric acid and borate can react with a suitable dihydroxy compound, to form the boric acid ester and the borate monoester, respectively.

These mechanisms are also consistent with the literature: Su and Suarez [44] have found evidence that trigonal and tetrahedral boron can form complexes on hydrous ferric oxide (HFO), and Peak et al. [45], using Attenuated Total Reflectance Fourier Transform

Fig. 6. Boron desorption cycles.

Infrared (ATR-FTIR) spectroscopy, have concluded that boric acid is adsorbed (on HFO surface) via both physical adsorption (outer-sphere) and inner-sphere reactions [45]. In seawater (average pH 8.3 and boron concentration of 4.2 mg L^{-1}), the dominant species is boric acid, so two possible interactions are proposed in Eqs. (13) and (14) when chiFer(III) is in contact with boron compounds. Thus, particularly for seawater, the first interaction (Eq. (13)) is probably the most active. In addition, a weak interaction between the boron species and the NH_2 groups of chitosan was previously reported by Demey et al. [40] and Gazi and Shahmohammadi [46].

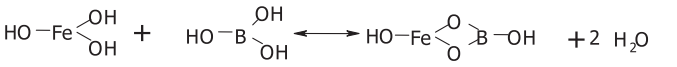

(13)

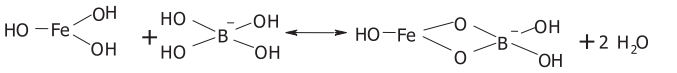

(14)

These mechanisms (Eqs. (13) and (14)) can only take place if the distances between adjacent OH^- groups in the $Fe(OH)_3$ structure are similar (or of the same order of magnitude) to those observed for boric acid (and borate ions) [40]. Consequently, desorption may be performed under basic medium via basic hydrolysis of esters (in the presence of OH^- groups) and via the repulsion between the negatively charged surface of chiFer(III) and the boron anion species (at pH > 9.2 the predominate species is $B(OH)_4^-$).

Additionally, the final pH and iron concentration of the seawater effluent (after adsorption) were monitored continuously: pH did not change through the column (final pH was 8.3), and no iron concentration and no precipitate were detected in the residual effluent, which suggested good stability of the chiFer(III) material in the continuous adsorption system with seawater.

4. Conclusions

This study presents the synthesis of a new low-cost chitosan/$Fe(OH)_3$-based sorbent and the results of its application for boron recovery from seawater. SEM-EDX analysis revealed a homogenous distribution of iron(III) hydroxide in whole material and porosity studies confirmed that chiFer(III) is a mesoporous material. The sorbent was found to be stable in the continuous system with seawater. Column studies demonstrated the re-usability of chiFer(III): regeneration can be performed with water (at pH 12) as eluent, which is a potential advantage over expensive commercial resins. The molar ratio between mass of adsorbed boron (in the five consecutive cycles) and mass of iron(III) hydroxide present in the adsorbent was 10.7 $mmol_B \cdot (mol_{Fe(OH)_3})^{-1}$. The Thomas, Yoon and Nelson, and Bohart–Adams models adequately fit the experimental data.

Acknowledgements

This work was supported by the Spanish Ministry of Economy and Competitiveness, MINECO (Project No. CTQ 2011-22412). The authors would like to thank to Mr. A. Brun and Mrs. C. Balieu (from the École des Mines d'Alès-France), and Dr. A. Fortuny and Dr. M.T. Coll (from the Polytechnic University of Catalonia, Spain) for their assistance in this project.

References

[1] World Health Organization, Guidelines for drinking-Water quality, fourth ed., Geneva, 2011.
[2] N. Ostürk, D. Kavak, T. Ennil, Boron removal from aqueous solution by reverse osmosis, Desalination 223 (2008) 1–9.
[3] N. Hilal, G.J. Kim, C. Somerfield, Boron removal from saline water: a comprehensive review, Desalination 273 (2011) 23–35.
[4] S. Karahan, M. Yurdakoç, Y. Seki, K. Yurdakoç, Removal of boron from aqueous solutions by clays and modified clays, J. Colloid Interface Sci. 293 (2006) 36–42.
[5] N. Öztürk, D. Kavak, Adsorption of boron from aqueous solutions using fly ash: Batch and column studies, J. Hazard. Mater. B127 (2005) 81–88.
[6] M. Simonnot, C. Castel, M. Nicolai, C. Rosin, M. Sardin, H. Jauffret, Boron removal from drinking water with a boron selective resin: is the treatment really selective?, Water Res 34 (2004) 109–116.
[7] N. Kabay, S. Sarp, M. Yuksel, M. Kitis, H. Koseoglub, Ö. Arar, M. Bryjak, R. Semiat, Removal of boron from SWRO permeate by boron selective ion exchange resins containing N-methylglucamine groups, Desalination 223 (2008) 49–56.
[8] D. Prats, M.F. Chillon-Arias, M. Rodriguez-Pastor, Analysis of the influence of pH and pressure on the elimination of boron in reverse osmosis, Desalination 128 (2000) 269–273.
[9] M. Rodríguez-Pastor, A. Ferrándiz-Ruiz, M.F. Chillon, D. Prast-Rico, Influence of pH in the elimination of boron by means of reverse osmosis, Desalination 140 (2001) 145–152.
[10] Y. Cengeloglu, G. Arslan, A. Tor, I. Kocak, N. Dursun, Removal of boron from water by using reverse osmosis, Sep. Purif. Technol. 64 (2008) 141–146.
[11] Z. Yazicigil, Y. Oztekin, Boron removal by electrodialysis with anion-exchange membranes, Desalination 190 (2006) 71–78.
[12] T. Itakura, R. Sasai, H. Itoh, Precipitation recovery of boron from wastewater by hydrothermal mineralization, Water Res. 39 (2005) 2543–2548.
[13] A. Erdem, A. Yilmaz, R. Boncukcuoğlu, M. Muhtar-Kocakerim, A quantitative comparison between electrocoagulation and chemical coagulation for boron removal from boron-containing solution, J. Hazard. Mater. 149 (2007) 475–481.
[14] H. Demey, M. Ruiz, J.A. Barron-Zambrano, A.M. Sastre, Boron removal from aqueous solutions using alginate gel beads in fixed bed systems, J. Chem. Technol. Biot., in-press, Doi: 10.1002/jctb.4361.
[15] M. Ruiz, C. Tobalina, H. Demey-Cedeño, J.A. Barron-Zambrano, A.M. Sastre, Sorption of boron on calcium alginate gel beads, React. Funct. Polym. 73 (2013) 635–657.
[16] M. Ruiz, L. Roset, H. Demey, S. Castro, A.M. Sastre, J.J. Pérez, Equilibrium and dynamic studies for adsorption of boron on calcium alginate gel beads using principal component analysis (PCA) and partial least squares (PLS), Mat. -wiss. U. Werkstofftech. 44 (2013) 410–415.
[17] O.P. Ferreira, S.G. de Moraes, N. Duran, L. Cornejo, O.L. Alves, Evaluation of boron removal from water by hydrotalcite-like compounds, Chemosphere 62 (2006) 80–88.
[18] P. Koilraj, K. Srinivasan, High sorptive removal of borate from aqueous solution using calcined ZnAl layered double hydroxide, Ind. Eng. Chem. Res. 50 (2011) 6943–6951.
[19] T. Yoshioka, T. Kameda, M. Miyahara, M. Uchida, T. Mizoguchi, A. Okuwaki, Removal of tetrafluoroborate ion from aqueous solution using magnesium–aluminum oxide produced by the thermal decomposition of a hydrotalcite-like compound, Chemosphere 69 (2007) 832–835.
[20] M. Zhang, E.J. Reardon, Removal of B, Cr, Mo, and Se from wastewater by incorporation into hydrocalumite and ettringite, Environ. Sci. Technol. 37 (13) (2003) 2947–2952.
[21] F.L. Theiss, G.A. Ayoko, R.L. Frost, Removal of boron species by layered double hydroxides: a review, J. Colloid Interface Sci. 402 (2013) 114–121.
[22] M. Turek, P. Dydo, J. Trojanowska, A. Campen, Adsorption/co-precipitation – reverse osmosis system for boron removal, Desalination 205 (2007) 192–199.
[23] H.C. Thomas, Heterogeneous ion exchange in a flowing system, J. Am. Chem. Soc. 66 (1944) 1664–1666.
[24] Y.H. Yoon, J.H. Nelson, Application of gas adsorption kinetics. I. A theoretical model for respirator cartridge service life, Am. Ind. Hyg. Assoc. J. 45 (1984) 509–516.
[25] A.E. Yilmaz, R. Boncukcouglu, M.T. Yilmaz, M.M. Kocakerim, Adsorption of boron from boron-containing wastewaters by ion exchange in a continuous reactor, J. Hazard. Mater. B117 (2005) 221–226.
[26] G.S. Bohart, E.Q. Adams, Some aspects of the behaviour of charcoal with respect to chlorine, J. Am. Chem. Soc. 42 (1920) 523–544.
[27] M. Ruiz, A.M. Sastre, M.C. Zikan, E. Guibal, Palladium sorption on glutaraldehyde-crosslinked chitosan in fixed-bed systems, J. Appl. Polym. Sci. 81 (2001) 153–165.
[28] E. Guibal, A. Larkin, T. Vincent, J.M. Tobin, Chitosan sorbents for platinum sorption from dilute solutions, Ind. Eng. Chem. Res. 38 (1999) 401–412.
[29] K.S.W. Singh, D.H. Everett, R.A.W. Haul, L. Moscou, R.A. Pierotti, J. Rouquerol, T. Siemieniewska, Reporting physisorption data for gas/solid systems with special reference to the determination of surface area and porosity, Pure Appl. Chem. 57 (1985) 603–619.
[30] S. Brunauer, P.H. Emmet, E. Teller, Adsorption of gases in multimolecular layers, J. Am. Chem. Soc. 60 (1938) 309–319.

[31] E.P. Barret, L.G. Joyner, P.P. Halenda, The determination of pore volume and area distributions in pourous substances. I. Computations from nitrogen isotherms, J. Am. Chem. Soc. 73 (1951) 373–380.
[32] I. Yilmaz-Ipek, N. Kabay, M. Yuksel, Modeling of fixed bed column studies for removal of boron from geothermal water by selective chelating ion exchange resins, Desalination 310 (2013) 151–157.
[33] B. Kiran, A. Kaushik, Cyanobacterial biosorption of Cr (VI): Application of two parameter and Bohart Adams models for batch and column studies, Chem. Eng. J. 144 (2008) 391–399.
[34] J. Barron-Zambrano, A. Szygula, M. Ruiz, A.M. Sastre, E. Guibal, Biosorption of reactive black 5 from aqueous solutions by chitosan: column studies, J. Environ. Manage. 91 (2010) 2669–2675.
[35] A. Ayala, L. Serna, E. Mosquera, Freeze-drying in yellow pitahaya (*Selenicereus megalanthus*), Vitae, Revista de la facultad de química farmacéutica 17 (2010) 121–127.
[36] V.P. Oikonomopoulou, M.K. Krokida, V.T. Karathanos, The influence of freeze drying conditions on microstructural changes of food products, Proc. Food Sci. 1 (2011) 647–654.
[37] T. Ennil-Köse, N. Öztürk, Boron removal from aqueous solutions by ion-exchange resin: colums sorption–elution studies, J. Hazard. Mater. 155 (2008) 744–749.
[38] M. Badruk, N. Kabay, M. Demircioğlu, H. Mordoğan, U. Ipekoğlu, Removal of boron from wastewater of geothermal power plant by selective ion-echange resin. II. Column sorption–elution studies, Sep. Sci. Technol. 34 (1999) 2981–2995.
[39] N. Kabay, S. Sarper, M. Yuksel, Ö. Arar, M. Bryjak, Removal of boron from seawater by selective ion exchange resins, React. Funct. Polym. 67 (2007) 1643–1650.
[40] H. Demey, T. Vincent, M. Ruiz, A.M. Sastre, E. Guibal, Development of a new chitosan/$Ni(OH)_2$-based sorbent for boron removal, Chem. Eng. J. 244 (2014) 576–586.
[41] M. Pagznl, D. Lemarchand, A. Spivack, J. Gaillardet, A critical evaluation of the boron isotope pH proxy: The accuracy of ancient ocean pH estimates, Geochim. Cosmochim. Acta 69 (4) (2005) 953–961.
[42] G. Zelmanov, R. Semiat, Boron removal from water and its recovery using iron (Fe^{+3}) oxide/hydroxide-based nanoparticles (NanoFe) and NanoFe-impregnated granular activated carbon as adsorbent, Desalination 333 (2014) 107–117.
[43] B. Wang, X. Guo, P. Bai, Removal technology of boron dissolved in aqueous solutions – a review, Colloids Surf. A 444 (2014) 338–344.
[44] C. Su, C. Suarez, Coordination of adsorbed boron: a FTIR spectroscopic study, Environ. Sci. Technol. 29 (1995) 302–311.
[45] D. Peak, G.W. Luther, D.L. Sparks, ATR-FTIR spectroscopic studies of boric acid adsorption on hydrous ferric oxide, Geochim. Cosmochim. Acta 67 (14) (2003) 2551–2560.
[46] M. Gazi, S. Shahmohammadi, Removal of trace boron from aqueous solution using iminobis-(propylene glycol) modified chitosan beads, React. Funct. Polym. 72 (2012) 680–686.